Derivatized chitosan-oil-in-water nanocapsules for *trans*-cinnamaldehyde delivery

Serena Berberolli[‡ab], Mar Collado-González[‡cd*], Yadira González-Espinosa[e], Gurmeet Kaur[f], Priyanka Sahariah[g*], and Francisco M. Goycoolea*[h]

[‡]These authors have contributed equally

[a] Department of Biomolecular Science, University of Urbino, Carlo Bo, Piazza del Risnascimento, 6, 61029 Urbino, PU, Italy

[b, d-f, h] School of Food Science and Nutrition, University of Leeds, Leeds, UK, LS2 9JT

[c] Department of Cell Biology and Histology, University of Murcia, 30100 Murcia, Spain

[g] Biomedical Centre, University of Iceland, 16, Vatnsmýrarvegur, 101 Reykjavík, Iceland

[a]S.Berberolli@gmail.com, [c]mdmcg1@um.es, [e]Y.Gonzaleze@hotmail.com, [f]gurmeet.Kaur1000@gmail.com, [g]prs@chemrsc.org, [h]F.M.Goycoolea@leeds.ac.uk

Highlights

O/w chitosan derivatives-coated nanocapsules preparation by spontaneous emulsification.

Chitosan-coated nanocapsules show 99 % *trans*-cinnamaldehyde association efficiency

N-hexanoyl-*N',N',N'*-trimethyl chitosan-coated nanocapsules are stable in PBS for 24 h.

*Authors for correspondence

Abstract

Trans-cinnamaldehyde, known for its bacterial anti-quorum sensing activity when applied at sublethal concentrations, has gained traction given its potential use against multidrug resistant bacteria. In this work, *trans*-cinnamaldehyde-loaded oil-in-water nanocapsules coated with chitosan, *N*,*N*,*N*-trimethyl chitosan chloride, *N*-(2-(*N*,*N*,*N*-trimethylammoniumyl)acetyl) chitosan chloride or *N*-(6-(*N*,*N*,*N*-trimethylammoniumyl)hexanoyl)chitosan chloride were obtained. All the formulated nanocapsules showed a Z-average hydrodynamic diameter ~160 nm and ζ-potential higher than +40 mV. *N*,*N*,*N*-trimethyl chitosan-coated oil-in-water nanocapsules showed the greatest *trans*-cinnamaldehyde association efficiency (99.3 ± 7.6) % and total payload release (88.6 ± 22.5) %, while *N*-(6-(*N*,*N*,*N*-trimethylammoniumyl)hexanoyl)chitosan chloride chitosan-coated oil-in-water nanocapsules were the only formulations stable in phosphate buffer saline PBS (pH 7.4) upon incubation at 37 ˚C for 24 h. Future work should address the stability of the developed nanocapsules in culture media and their biological performance.

KEYWORDS: Chitosan, oil-in-water nanocapsules, *trans*-cinnamaldehyde, stability, dynamic light scattering, bacterial quorum sensing.

1. Introduction

Trans-cinnamaldehyde (*t*CA) is a phenylpropanoid obtained from cinnamon and C*assia* essential oils [1]. The interest on *t*CA lies in its antifungal [2] and antibacterial [3] quorum sensing inhibitory [4] activities, among others [5]. It has been reported that *t*CA shows a synergistic effect when administered together with polymyxin B against *Serratia marcescens* [6] and when administered together with colistin against *Pseudomonas aeruginosa* [7]. *t*CA alone or in synergistic blends could be an alternative treatment to fight against bacterial infections specially when fighting against multidrug resistant bacteria species. At low concentrations, commonly in the μM range [5], *t*CA is a well-established quorum sensing (QS) inhibitor of Gram-negative bacteria [8]. QS are bacteria-density dependent communication systems that induce virulence genes expression, such as those involved in biofilm production, bioluminescence, among other traits [9,10]. It has been reported that *t*CA exert pleiotropic effects on QS, thus reducing the virulence factors expressed by Gram-negative bacteria [8,11]. In addition, it has been reported that the *t*CA QS inhibition ability against *Pseudomonas aeruginosa* increased when combined with colistin or tobramycin [7], which suggests an increase in the sensitivity against antibiotics when they are co-applied with *t*CA. Given this capacity combined with the interference with QS, *t*CA may offer a promising potential to fight against multi-resistant bacteria.

The partition coefficient (logP) reported for *t*CA is 1.98 [12], which means that it shows low water solubility, namely 1.4 mg/mL [13]. Oil-in-water nanoemulsion (NE) have been proposed as a strategy to increase *t*CA water solubility and bioavailability [14]. However, NE show low stability, which compromises their beneficial properties. Coating NE with oppositely charged polyelectrolytes confers it with electrostatic colloidal stability, further here referred to it as oil-in-water nanocapsules (o/w NC). To increase the interactions

between o/w NC and mucosal surfaces, cell membranes and bacterial surfaces, polycationic polymers, such as Eudragit® [15,16] or chitosan [17], among others, have been used as coating polyelectrolytes.

Chitosan (CS) is a family of aminopolysaccharides that shows interesting properties for the development of drug delivery systems such as mucoadhesion, immunomodulatory effect, antibacterial [18] and anti-QS properties [19]. Chitosan coating results in positively charged o/w nanocapsules that will interact easily with negatively charged bacterial and mammalian cells surfaces [20,21]. *t*CA-loaded CS-coated o/w NC have been successfully prepared by our research group [1]. We demonstrated that the tCA-loaded NC can target an *E. coli* Top 10 strain QS reporter and inhibited QS more effectively than non-CS coated NE. These nanocapsules can bind to *E. coli* bacteria under a "stoichiometric ratio" [21]. In other studies, we have shown the efficacy of the nanocapsules to load baicalein, quercetin, and naringenin to inhibit bacterial QS and biofilm formation [22,23]. Given that CS has a pKa of 6.0 ± 0.1 [24], it loses its polycationic nature at neutral pH. To overcome this limitation and obtain polycationic CS at pH close to various relevant physiological and biological context, side groups such as quaternary ammoniumyl have been added to CS to yield quaternary ammonium CS derivatives with polycationic character at a wide range of pH. Sahariah and colleages have shown that these derivatives interact effectively with negative membranes of bacteria at neutral pH, which increases their antibacterial activity [25] under physiological conditions. The anti-QS of such chitosan derivatives in solution or in nanostructured particle formulations has not been reported. As a first step to address this gap, we have hypothesized in this work that o/w NC coated with CS quaternary ammonium derivatives and loaded with *t*CA will exhibit improved physicochemical and colloidal stability properties which will translate into novel antimicrobial approaches. In this work, we

formulated *t*CA-loaded quaternary ammonium CS derivative-coated o/w NC using synthesized quaternary ammoniumyl CS derivatives having different spacers- *N,N,N*-trimethyl chitosan chloride (CSder1), *N-(2-(N,N,N*-trimethylammoniumyl)acetyl)-chitosan chloride (CSder2) and *N-(6-(N,N,N*-trimethylammoniumyl)hexanoyl)-chitosan chloride (CSder3) (Fig. 1). We report the synthesis of the chitosan derivatives using a novel synthetic methodology to obtain highly N-selective products. We report here, for the first time, the feasibility to formulate *t*CA-loaded NC,their thorough biophysical characterization and the evaluation of their colloidal stability in PBS at 37 °C up to 24 h, that enable to assess the suitability of these systems for following up studies aiming to assess their biological performance.

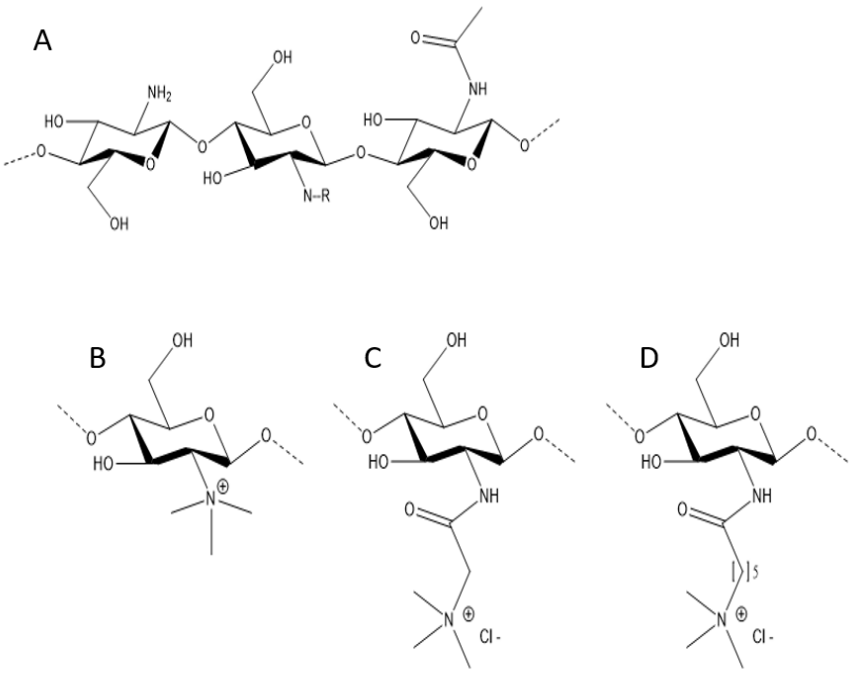

Fig. 1. Structure of partially deacetylated chitosan with side chain designated as R (A). The units with the side chains for chitosan (A), *N,N,N*-trimethyl chitosan chloride (B), *N-(2-(N,N,N*-trimethylammoniumyl)acetyl)-chitosan chloride (C) and *N-(6-(N,N,N*-trimethylammoniumyl)hexanoyl)-chitosan chloride (D) are also plotted.

2. Materials and methods

2.1. Materials

Chitosan HMC 90/5 (Batch number 212-181115-04) with a degree of acetylation (DA) ~5 %, as determined by ^{1}HNMR spectroscopy, and molar mass ~20.1 kg/mol, and polydispersity (Đ) 1.8 as determined by GPC-MALS-DRI, was from Heppe Medical Chitosan GmbH (Halle, Germany). Quaternary ammonium CS derivatives were synthesized and characterized in collaboration with the Department of Life and Environmental Sciences, University of Iceland (Reykjavik, Iceland). The molar mass distribution of the quaternary ammonium CS derivatives was characterized by asymmetrical flow field-flow fractionation (FFF multiflow AF2000 from Postnova Analytics GmbH, Landsberg am Lech, Germany) (Table 1 and Fig. S1 and S2). The degree of substitution (DS) for all the derivatives was determined by using the integrals in the ^{1}H NMR spectrum and are included in Table 1. ^{1}H-NMR spectra were recorded at 300 K using a Bruker Avance 300 MHz spectrometer equipped with a BBO probe. Samples were measured in D_2O at a concentration of 6 mg/mL. The final spectrum was processed using MestReNova software version 14.2.0-26256. The DS for the chitosan derivatives was calculated using the following equations:

$$DS\ for\ CSder1 = \left[\frac{\int(N - CH_3)}{\int(H_2 - H_6)}\frac{6}{9}\right] \cdot 100 \quad \text{(Eq 1)}$$

$$DS\ for\ CSder2\ and\ CSder3 = \left[\frac{\int(N - CO - CH_2)}{\int(H_2 - H_6)}\frac{6}{2}\right] \cdot 100 \quad \text{(Eq 2)}$$

Note: H2–H6 represent the protons H2, H3, H4, H5 & H6 in the glucosamine unit.

*t*CA (Mw = 132.6 g/mol, 99 % richness, density 1.08 g/mL) was purchased from Sigma-Aldrich (UK). Lecithin (Epikuron 145 V) was purchased from Cargill Texturizing Solutions GmbH (Hamburg, Germany) and stored at -20 ºC until use. Miglyol 812® was purchased from IOI OLEO GmbH (Witten, Germany). Acetonitrile and water were HPLC

grade and were purchased from Fisher Chemical (UK). 0.01 M phosphate buffer saline (PBS) tablets (pH 7.4) were purchased from Fischer BioReagents (Belgium, code: BP2944-100). Absolute ethanol was purchased from VWR. MilliQ water (resistivity = 18.2 mΩ) was also used. All chemicals used in synthesis were purchased from Sigma-Aldrich.

2.2. Methods

2.2.1. Synthesis

Chitosan hydrochloride salt. Chitosan (DA ~5%, Mw ~2 x 10^4 g/mol) was stirred in hydrochloric acid 37 % at 0.06 g/mL until fully dissolved. The solvent was removed under reduced pressure. The solid was triturated with 20 mL of acetonitrile twice and redissolved in water (100 mL) and lyophilized to obtain the final product that will be used for further modification. Yield: 3.6 g (98%).

CSder1. Chitosan hydrochloride (1 g, 4.63 mmol) was dissolved in DMSO (30 mL), followed by addition of 10.02 mmol of $NaHCO_3$. 25.06 mmol of methyl iodide was then added dropwise to the reaction and the mixture was stirred at 50 °C for 48 h. The reaction mixture was diluted with 20 mL de-ionized water and purified using dialysis membrane (3.5 kDa Mw cut-off). The solution was ion-exchanged against 10% NaCl and re-dialyzed against water for 24 h and then lyophilized. Yield: 0.96 g (79.3%). ^{1}H NMR (300 MHz, D_2O): δ 2.10 (N-Ac), 3.37 [$N(CH_3)_3$], 3.57 [6-O-CH_3],, 3.77−4.49 (H-2−H-6), 5.49 (H-1) ppm.

CSder2. Chitosan hydrochloride (1 g, 4.63 mmol) was dissolved in DMSO (30 mL), followed by addition of 10.02 mmol of Cs_2CO_3. 25.06 mmol of Bromoacetyl chloride was then added dropwise to the reaction and the mixture was stirred at 50°C for 48 h. After completion, the product was precipitated by diluting with de-ionized water (30 mL), filtered and washed with 20 mL of acetonitrile twice. The precipitate was then stirred in

25 mL of trimethylamine solution 31-35 wt. % in ethanol at room temperature for 24 h. The reaction mixture was then diluted with de-ionized water, dialyzed and lyophilized as described above to obtain CSder2. Yield: 1.18 g (79.1%). ^{1}H NMR (300 MHz, D_2O): δ 2.07 (N-Ac), 3.35 [$N(CH_3)_3$], 3.53−3.85 (H-2−H-6), 4.20 (CO-CH_2), 4.65 (H-1) ppm.

CSder3. Chitosan hydrochloride (1 g, 4.63 mmol) was dissolved in DMSO (30 mL), followed by addition of 10.02 mmol of Cs_2CO_3. 25.06 mmol of 6-bromohexanoyl chloride was then added dropwise to the reaction and the mixture was stirred at 50°C for 48 h. After completion, the precipitation and following treatments were as described above to obtain CSder3. Yield: 1.25 g (70.6%). ^{1}H NMR (300 MHz, D_2O): δ 1.41 (N-CH_2-), 1.69 (-CH_2-), 1.84 (-CH_2-), 2.07 (N-Ac), 2.36 (CO-C-CH_2), 3.12 [$N(CH_3)_3$], 3.33−3.95 (H-2−H-6), 4.65 (H-1) ppm.

2.2.1. Preparation of oil-in-water nanocapsules

Oil-in-water nanocapsules were prepared following the spontaneous emulsification technique developed by Calvo and colleagues [26], with slight modifications: the method was down-scaled dividing by half all the volumes while keeping concentrations. To prepare blank CS-coated o/w NC, 100 µL of Epikuron 145V at 100 mg/mL in ethanol were mixed with 132.5 µL of ethanol and 31.5 µL of Miglyol 812®. On top of the solution obtained, 2.375 mL of ethanol was added to form the organic phase solution, which was later poured on the water phase under moderate magnetic stirring. Water phase consisted in 5 mL of CS or CS derivative solution, prepared at 0.5 mg/mL. (the first was prepared in 5 % stoichiometric excess of HCl whereas CS derivative solutions were prepared in MilliQ water). After mixing both phases by pouring the organic phase over the aqueous one, a milky solution was obtained. Ethanol was evaporated in rotavapor (HeidolphHei-Vap advantage, Heidolph Instruments GmbH & Co, KG, Denmark) at 40 ºC and rotating at 100 rpm. The pressure was set to 150 mbar for 5 minutes and then was lowered to 50

184 mbar for another 12 minutes keeping temperature and rotation. The final volume was 1
185 mL approximately. Then, another mL of MilliQ water was added to the formulation. To
186 prepare loaded o/w NC, the same procedure was applied with slight variations in the
187 preparation of the organic phase: instead of adding 132.5 μL of absolute ethanol, this
188 volume corresponded to a solution of *t*CA in ethanol at 75.6 mM. For the preparation of
189 NE, the water phase consisted only in MilliQ water.

190 2.2.2. Size and ζ-potential characterization

191 The hydrodynamic diameter distribution was measured by non-invasive back-scattering
192 (NIBS) dynamic light scattering (DLS) at an angle of 173°. The ζ-potential was
193 determined from the electrophoretic mobility by mixed-mode measurement phase
194 analysis light scattering (M3-PALS). Both parameters were measured using a Zetasizer
195 Ultra model zsu5700 (Malvern Pananalytical, Worcestershire, UK) equipped with a 4
196 mW He/Ne laser beam (λ = 633 nm). Each measurement corresponds to the average of 4
197 runs executed under automatic conditions. Prior to each analysis, the formulations were
198 diluted up to 5 % in only in MilliQ water for the size analysis and in 1 mM NaCl to
199 perform ζ-potential analysis measurements. Both parameters were measured at 25 ºC.

200 2.2.3. Morphology

201 Transmission electron microscopy (TEM) analysis was carried out using a transmission
202 electron microscope JEOL JEM-1400. A droplet of the o/w NC under analyses was
203 deposited on a copper grid carbon coated. Then, the excess of liquid was removed, and
204 the sample was allowed to dry. The images were captured at 100 kV.

205 2.2.4. Encapsulation efficiency and loading capacity

206 *Trans*-cinnamaldehyde content in each o/w NC or NE solution was analyzed by HPLC.
207 The stationary phase was a C18 Kinetex column (Kinetex 5 µm C188 100 Å, LC column
208 150 x 4.6 mm, H18-045285, 5701-0054). The flow rate was set to 0.6 mL/min and the
209 signal from UV – detector set online were recorded for 20 min. Water (A) and acetonitrile
210 (B) were used as mobile phases in gradient mode: 0-10 min 70 % A and 30 % B, 10-16
211 min 50 % A and 50 % B, 16-19 min 70 % A and 30 % B. The *t*CA was detected at λ =
212 285 nm. The volume injected for each analysis was 5 µL. The results shown are the
213 average of 3 different injections carried out at the same conditions.

214 A calibration curve was performed for the analysis of *t*CA solutions in ethanol at
215 concentration in the range 0.005 to 4 mM, following the methodology explained above.
216 From the chromatograms obtained at λ =285 nm, the area under the curve (AUC) of the
217 peak eluted at around 3.5 min was analyzed. The calibration curve was created plotting
218 AUC against concentration (in M). The R^2 was 0.9999. The calibration curve function
219 was AUC=2451.4 x concentration – 16.135.

220 For the determination of encapsulation efficiency, 1 mL of each o/w NC formulation was
221 centrifuged at 25000 g for 60 minutes at 15 ºC in a high-speed centrifuge (Beckmann
222 culter Avanti j-30I). This process allows the separation of the sample in three phases: a
223 top creamy layer containing o/w NC, a pellet consisting on the exceeding components
224 complexed together and between those previously indicated, a subnatant containing
225 uncomplexed components in free solution. The creamy phase was collected and placed in
226 separate tube and filled with water up to one mL. Then, 25 µL of the solution prepared
227 was added in 475 µL of ethanol and centrifuged at 2200 g for 5 minutes at room
228 temperature in a centrifuge (5418, Eppendorf, Germany). The amount of *t*CA was
229 determined by HPLC, as indicated above. The encapsulation efficiency (EE%) was
230 determined as percentage of *t*CA in the creamy phase ($c_{o/w\,NC}$) with respect to the total

concentration of the payload added in the formulation (c_{total}), according to the equation 3.

$$EE\ (\%) = \frac{\left(c_{o/w\ NC} x100\right)}{c_{total}} \quad \text{(Eq. 3)}$$

It was calculated the loading capacity (LC %) of different o/w NC as the percentage of mass of entrapped *t*CA ($m_{entrapped\ tCA}$) with respect to the total mass of the o/w NC ($m_{o/w\ NC}$), according to the equation 4.

$$LC\ (\%) = \frac{m_{entrapped\ tCA} x100}{m_{o/w\ NC}} \quad \text{(Eq. 4)}$$

2.2.5. *In vitro t*CA release

The *in vitro* release test was carried out in PBS: 0.5 mL of o/w NC for each formulation was added to 4.5 mL of PBS solution and incubated for 6 h at 37 ºC. This was considered as an end-point measurement, based on our previous study [1]. To this end, 1.5 mL of each solution were placed in a Vivaspin tube 15 (Sartorius, UK, 30000 MWCO) and centrifuged at 3992 g for 20 min in a Rotina 380R centrifuge (Helttic Zentrifugen). The concentration of *t*CA in the filtered solution was determined by HPLC following the method described above. The *in vitro* release was calculated as percentage according to the equation 5:

$$In\ vitro \text{ release } (\%) = \frac{(c_{t\text{CA released}} x\ 100)}{c_{total}} \quad \text{(Eq. 5)}$$

Where $c_{t\text{CA released}}$ is the concentration of *t*CA quantified in the filtrated by HPLC.

2.2.6. Stability study

The stability of the o/w NC was evaluated in terms of size variation over time after incubation in PBS 0.01 M pH 7.4 at 37 ºC in order to evaluate the aggregation of the particles. 0.25 mL of each nanocapsules suspension were transferred into cuvettes containing 2.25 mL of PBS solution and the suspension was incubated at 37 ºC for 24 hours. The size of the o/w NC or NE by DLS was analyzed following the same method described above, at different time points: immediately after adding the o/w NC or NE to the PBS and then every hour up to 3 h and after 24 h of incubation.

2.2.7. Statistical analysis

Normal distribution of variables and homogeneity of variances were confirmed by Shapiro-Wilk and Levene tests, respectively. ANOVA one-way test followed by a Games Howell test were carried out to identify the significant differences among the characteristics studied on each data population. The significance level was fixed to 95 %. For statistical analyses SPSS software version 28.0.1.1. was used.

3. Results and discussion

Different approaches have been explored to overcome the low colloidal stability of NE formulations in certain instances. For example, inorganic particles, such as silica (SiO_2) nanoparticles, have been used to stabilize *t*CA NE forming Pickering emulsions [27]. Silica-coated *t*CA-loaded o/w NC showed antibacterial activity on gram positive (*S. aureus*) as well as on Gram-negative (*E. coli*, *P. aeruginosa* and *En. cloacae*) bacteria models and promoted cell proliferation of cells 3T3 [27]. Other strategies are based on the use of polycationic polymers for coating *t*CA-loaded o/w NC. Polycationic polymers are used to target the o/w NC against cell membranes and bacterial surfaces due to their negative charge. To this end, CS with Mw in the range ~1.15 x 10^5 g/mol and DA 10 % (from Sigma-Aldrich Co. Ltd) was used as stabilizing agent for *t*CA-loaded NE. The

resulting o/w NC showed a synergistic antibacterial effect between CS and *t*CA, namely 98 % on *S. aureus* and 96 % on *E. coli* bacterial strands when *t*CA applied was 17.1 and 34.2 μM, respectively [28]. In our previous work, CS (molar mass ~1.15 x 10^5 g/mol and DA ~42 %) that did not show antibacterial activity, was used to prepare *t*CA-loaded NC. This system showed anti-QS and no toxic activity against *E. coli* [1]. The inhibition of QS activity has been pursued as a strategy to inhibit the virulence of phenotypic factors such as the formation of biofilms, including multispecies biofilms. Thus, in principle, the inhibition of QS can serve to mitigate the virulence of a broad spectrum of bacterial species.

3.1.Preparation of chitosan derivatives

Quaternary ammonium chitosan derivatives significantly enhance the interaction of the polymer with the bacterial membrane as seen in previous studies. In this study, we synthesized a series of CS derivatives where the cationic functionality was incorporated into the amino group of the polymer backbone using various chain lengths. Previous studies on quaternization of the amino group of chitosan [29] reported the use of acidic medium or other heterogeneous medium resulting in low DS in the product. This has recently been overcome by use of protection groups where up to 100% DS is reported [30,31]. However, requirement of additional synthetic steps such as protection/deprotection combined with the significant degradation of the polymer backbone, puts limitations on this strategy. In this study, we report a direct method of functionalizing the amino group of CS using the hydrochloride salt of chitosan in organic medium to produce highly *N*-substituted product (Fig. 2). CSder1 was synthesized from CS hydrochloride salt using methyl iodide/$NaHCO_3$ in DMSO. We obtained a *N*-trimethylated product with DS= 89.2 % and small % of 6-O-methylation (at 3.5 ppm) [32]. Using similar conditions (Cs_2CO_3/DMSO) combined with the corresponding acid

296 chlorides we successfully performed N-acylation with different chain lengths- CSder2
297 and CSder3, followed by substitution of the terminal halide by a *N*-trimethyl group. The
298 DS obtained for the products CSder**2** & CSder**3** are 92.5 and 74.0 %, respectively (Table
299 1). The spectra for CSder**2** & CSder**3** derivatives do not show very significant 3-*O* or 6-
300 *O*-methyl peak in the region of 3.4-3.5 [32]. So, we can thus suggest that the method
301 mostly provides N-selective modification. Therefore, this synthetic method has the
302 advantage of direct modification in a homogeneous medium and can be used to produce
303 selective *N*-substituted products. The average molar mass for the derivatives is in the
304 range 1.3−6.9 x 10^4 g/mol and the dispersity (Đ) is around 1.1. Đ is a parameter that shows
305 variability in chitosan and other biopolymers. In previous studies, we have reported Đ
306 values for chitosan in the range from ~1.5 to ~2.0 [33]. Of note, the Đ value for the
307 commercial chitosan used in this work (HMC 95/100 Batch number 212-090914-01) to
308 formulate NCs was equal to 1.2, lower a value than found in previous studies. The low Đ
309 values also found also for the chitosan derivatives (Table 1), might be related with a
310 narrow molecular weight distribution of the parent chitosan in their synthesis.
311 We characterized the series of water-soluble CS derivatives using ^{1}H-NMR spectroscopy.
312 The corresponding spectrum for each compound with the assigned peaks, chemical shifts
313 and integrals are shown in Fig. 3.
314

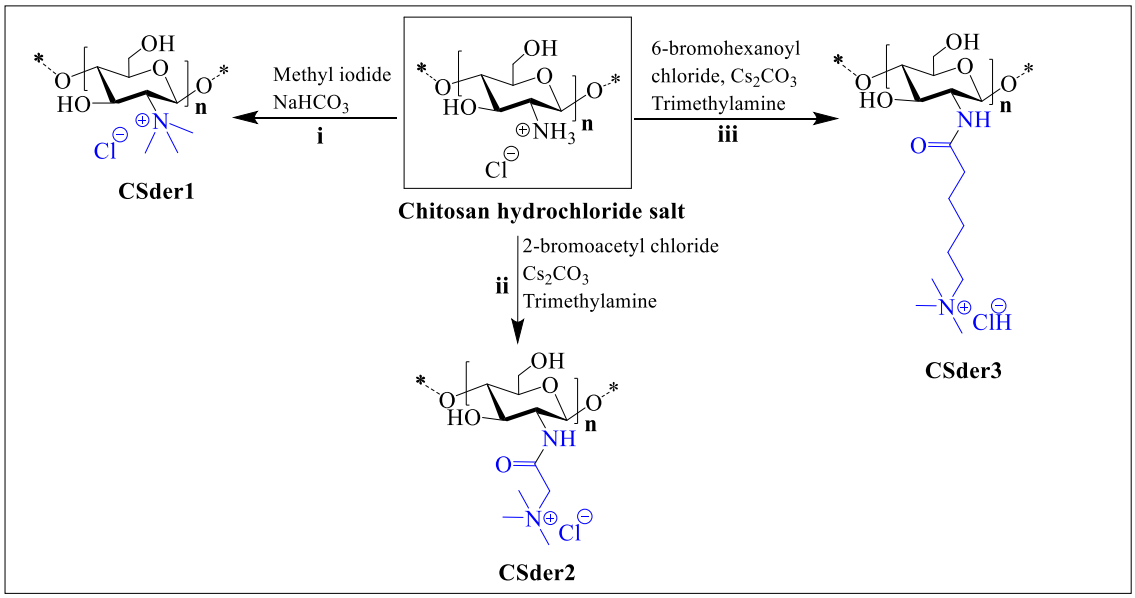

Fig. 2. Synthetic route for the quaternary ammonium chitosan derivatives (CSder1, CSder2 & CSder3) used in this work. Note: the degree of acetylation (5%) has been omitted for clarity in the structure.

Table 1. Physico-chemical properties of the synthesized chitosan derivatives.

	DA (%)	DS (%)	Mw (x10^4 g/mol)	Mn (x10^4 g/mol)	Đ (Mw/Mn)	Solubility
CSder1	5	89.2	1.27±0.04	1.19±0.01	1.07±0.02	water
CSder2	5	92.5	6.9±0.3	6.6±0.2	1.060±0.002	water
CSder3	5	74.0	2.04±0.06	1.78±0.05	1.15±0.01	water

DA = degree of acetylation; DS = degree of substitution (substituent groups are *N,N,N*-trimethyl, *N-(2-(N,N,N*-trimethylammoniumyl)acetyl) and *N-(6-(N,N,N*-trimethylammoniumyl)hexanoyl) for CSder1, CSder2 and CSder3, respectively); Mw & Mn = weight average molar mass and number average molar mass as determined by multidectection (MALS-DRI) asymmetric flow-field flow fractionation; Đ = dispersity

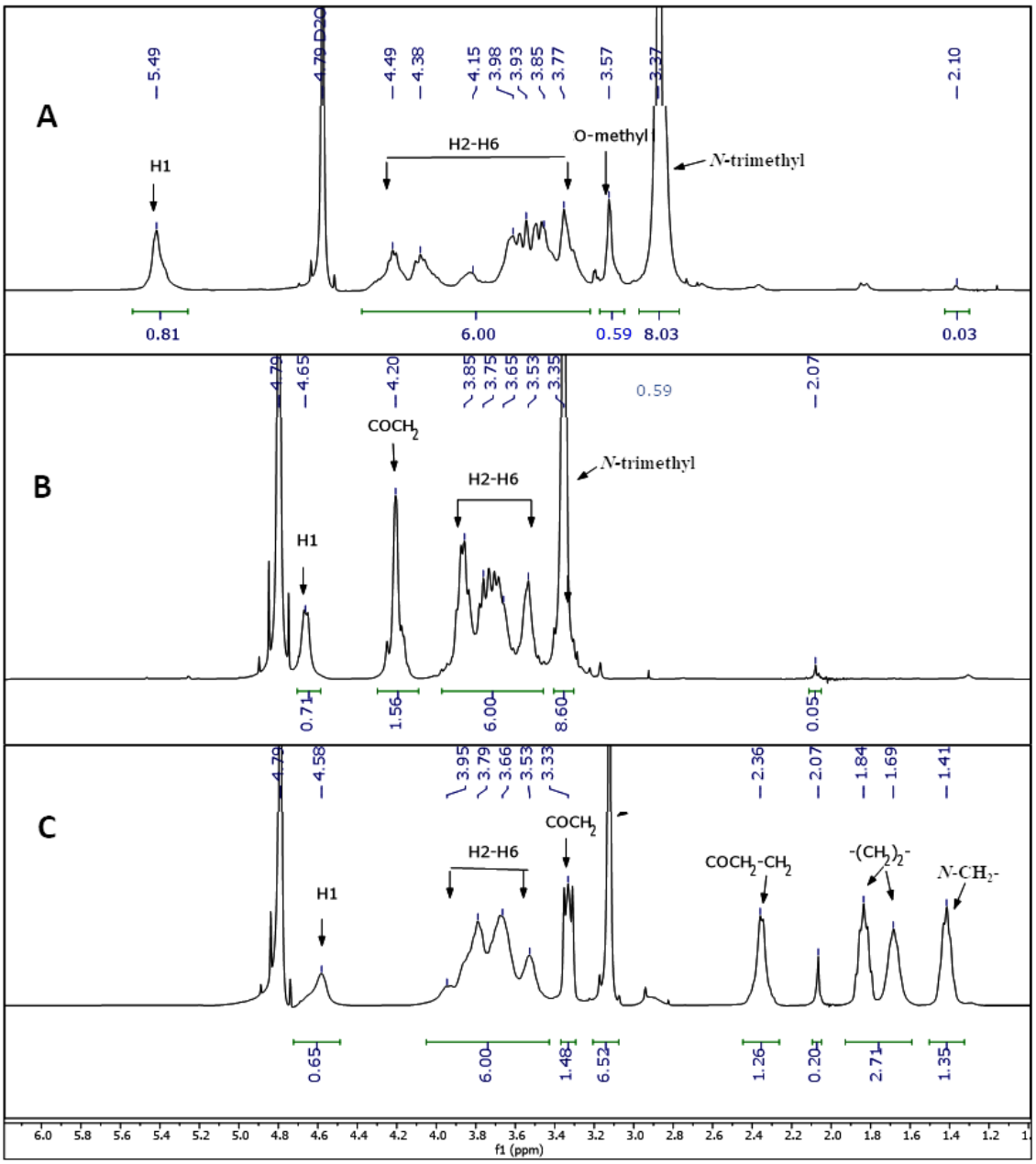

Fig. 3. Stacked ^{1}H-NMR spectra for the chitosan derivatives. A) CSder1, B) CSder2 and C) CSder3.

3.2.Oil-in-water nanocapsules: preparation and characterization

We utilized the three quaternary ammonium CS derivatives synthesized to prepare NCs and compared them with NCs prepared using a non-derivatised CS (DA ~5% and molar mass ~2 x 10^{4} g/mol).

3.2.1. Hydrodynamic characterization

Chitosan-coated o/w NC formulated in this work were monodisperse (PDI ≤~0.2) with droplet Z-average hydrodynamic diameter and ζ-potential values lying within a narrow range of ~156-166 nm ~+41-48 mV, respectively (Table 2 and Fig. 4). These results agree well with the physical characteristics of *t*CA-loaded CS-coated o/w NCs obtained by an identical protocol for spontaneous emulsification reported in our previous study [1], despite the differences in the CS characteristics used in the such study (*cf.* DA ~42 %, molar mass ~1.15 x 10^5 g/mol). The blank (non-loaded) o/w NC showed a hydrodynamic diameter equal to ~149 nm and ζ-potential equal to ~+50 mV, while *t*CA-loaded o/w NC showed a hydrodynamic diameter equal to ~165 nm and ζ-potential equal ~+42 mV [1]. However, in previous studies [34], we have reported that the overall size of the o/w NC depend on the properties of CS used for coating the NE droplets.

Table 2. Characteristics of *t*C-loaded and blank nanoemulsions and nanocapsules formulations.

Formulations[a]	Z-av. hydrodynamic diameter (nm)	PDI	pH	ζ-potential (mV)
BNE	179±14	0.21±0.02	4.1	-68 ± 3
PNE	162±11	0.20±0.02	4.6	-65 ± 4
PNC90/5	166±8	0.15±0.02	2.5	+46 ± 1
PNC1	162±24	0.07±0.02	4.2	+48 ± 3
PNC2	158±16	0.07±0.01	3.7	+41 ± 2
PNC3	156±17	0.11±0.02	4.4	+42 ± 2

[a]BNE = blank (non-loaded) NE; PNE = *t*CA-loaded NE; PNC90/5 = non-derivatized CS-coated *t*CA-loaded o/w NC; PNC1 = CSder1-coated *t*CA-loaded o/w NC; PNC2 = CSder2-coated *t*CA-loaded o/w NC; and PNC3 = CSder3-coated *t*CA-loaded o/w NC.

The hydrodynamic diameter of CS derivatives-coated *t*CA-loaded o/w NC was the same as the non-derivative-CS-coated *t*CA-loaded o/w NC, regardless the length of the side

chain. Regarding the differences in size between *t*CA-loaded NE and o/w NC, there seems to be a slight dependence on the length of the side chain of CS derivatives following the order CSder1 > CSder2 > CSder3 (Fig. 4D), thus suggesting that the longer the side chain is, the greater the reduction in the hydrodynamic size. Even when the observed differences in the Z-average hydrodynamic diameter values lie within the standard error of the DLS determinations, the overall size distribution curves (Fig. 4A) show discernible shifts on the higher tail end of the curve for the *t*CA-loaded NE with respect to the NCs coated with the CS derivatives, in keeping with a twice as large PDI values. Unexpectedly, although chitosan derivatives resulted in a size decrease of the NCs, the use of non-modified chitosan yielded a size increase of NCs (Fig. 4D), which agrees with the reported size increase of 6 nm [34] or 45 nm [1] of chitosan-coated NE.

Regarding the ζ-potential, all o/w NC showed a positive charge regardless the CS or CS derivative used for coating the NE (Table 2 and Fig. 4C). Of note, the use of CS derivatives, soluble at neutral pH, result in a similar pH than the pH of the NE suspension, with exemption of CSder2, that resulted in a pH decrease to 3.7. However, the need of acidic conditions to dissolve non-modified CS resulted in o/w NC suspension with pH equals to 2.5. This lower pH though, did not result in a noticeably different ζ-potential with respect to the other NCs prepared with CS derivatives.

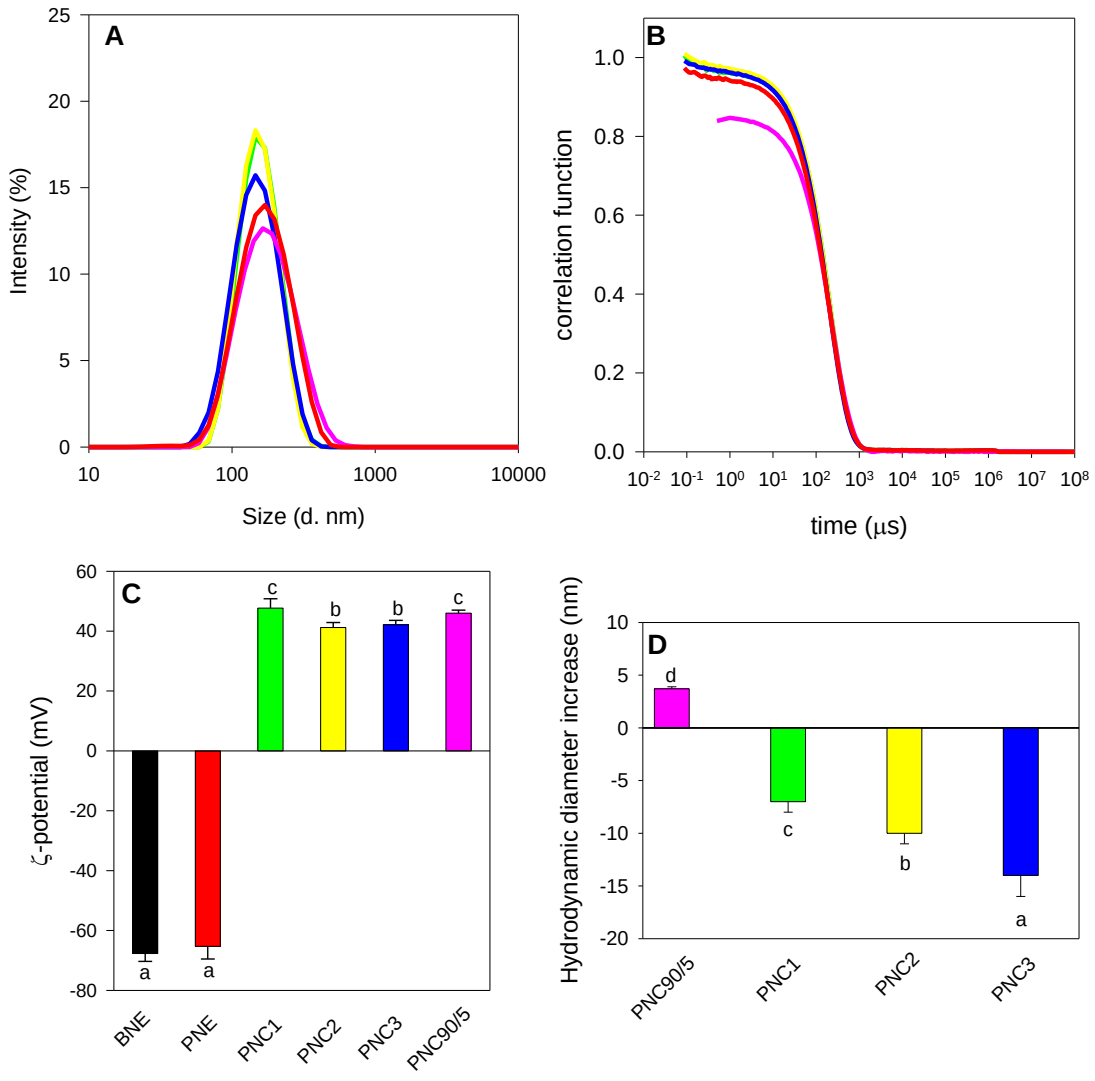

Fig. 4. Particle size distribution by intensity (A), correlation function (B), ζ-potential (C) and increment of the hydrodynamic diameter between *trans*-cinnamaldehyde-loaded nanoemulsion and *trans*-cinnamaldehyde-loaded nanocapsules (D). Lines and bars in the Fig.s correspond to *trans*-cinnamaldehyde-loaded nanoemulsions (PNE, red) or *trans*-cinnamaldehyde-loaded nanoemulsions coated with non-derivatised CS (PNC90/5, pink), CSder1 (PNC1, green), CSder2 (PNC2, yellow) and CSder3 (PNC3, blue) and unloaded nanoemulsion (BNE, black). Statistical differences ($p \leq 0.05$) are indicated with different numbers.

3.2.2. TEM imaging

All the o/w NC were spherical in shape as it became evident by TEM imaging (Fig. 5), in agreement with results reported previously for the morphology analysis of o/w NC [28,35]. Upon close inspection of the images, slight surface topological differences can be appreciated between the NCs coated with native CS with respect to those coated with the quaternized amine derivatives. It is interesting to note that the CSder2–coated NCs appear with heterogeneously distributed spots, not visible on the other imaged systems. Whether this peculiar topology stems on a heterogenous coating of the surface by this CS-derivative, remains to be further investigated.

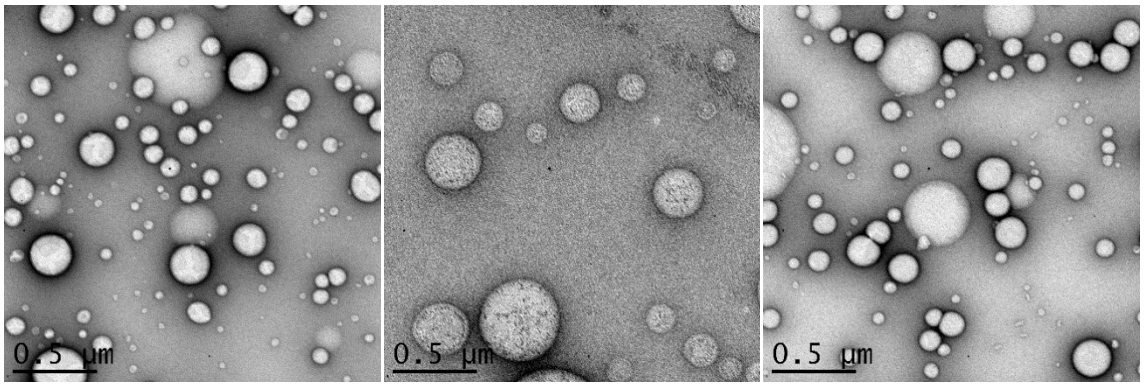

Fig. 5. TEM images of *t*CA-loaded o/w NC coated with CS (left), CSder2 (center) and CSder3 (right). The scale bar represents 0.5 µm in all images.

3.2.3. Encapsulation efficiency, loading capacity and in vitro release

The concentration of *t*CA was determined on the supernatant phase formed in nanoemulsions after being centrifuged. The encapsulation efficiency was then calculated. As can be seen in the Fig. 6, CSder1-coated *t*CA-loaded o/w NC showed the significantly higher ($p<0.05$) percentage of *t*CA loaded (99 ± 8 %) than the rest of the formulations. The amount of encapsulated *t*CA by o/w NC coated with CSder2 (37 ± 1 %) or CSder3 (38 ± 1 %) was not significantly different compared to the loaded o/w NC coated with the underivatised CS (28 ± 4 %). Regarding to the *t*CA loading capacity (%), CSder1-coated *t*CA-loaded o/w NC showed the significantly higher ($p<0.05$) percentage of *t*CA loading (2.9 ± 0.2 %) than the rest of the formulations. The amount of loaded *t*CA by o/w NC

401 coated with CSder2 (1.10 ± 0.03 %) or CSder3 (1.15 ± 0.03 %) was not significantly
402 different than the loading capacity in the underivatized CS-coated *t*CA-loaded o/w NC
403 (0.8 ± 0.1 %). The encapsulation efficiency and loading capacity values reported in this
404 work are in good agreement to the results reported in our previous study [1], who reported
405 an EE equal to 37 % and 82 % when preparing o/w NC using a 20 mM and 10 mM *t*CA,
406 respectively, and a loading capacity equal to 5.5 and 5.8 %, in the same order. We have
407 not at this stage a plausible explanation for the overall greater encapsulation efficiency
408 and loading capacity of the NCs formulated using the CSder1. However, it is a result that
409 underscores an important techno-functional advantage of these formulations over those
410 made using native CS or the other quaternized ammonium CS derivatives.

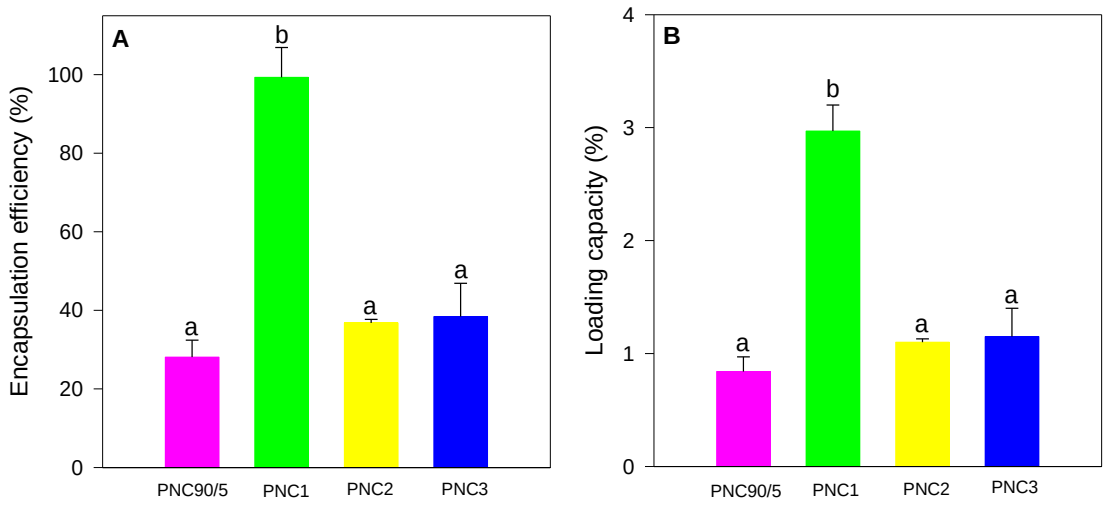

411

412 Fig. 6. Encapsulation efficiency (A) and Loading capacity (B) of o/w NC coated with
413 chitosan (PNC90/5), CSder1 (PNC1), CSder2 (PNC2) and CSder3 (PNC3). Statistical
414 differences ($p \leq 0.05$) are indicated with different numbers.

415 The CSder1-coated o/w NC showed better *t*CA in vitro release (89 ± 23 %) than the o/w
416 NC coated with non-modified CS (47 ± 6 %). The release from the other o/w NC coated
417 with CSder2 and CSder3 showed lower *t*CA release when compared to the non-CS-coated
418 o/w NC, namely (35 ± 2 %) and (29 ± 1 %), respectively (Fig. 7). There were no
419 significant differences among each o/w NC formulations.

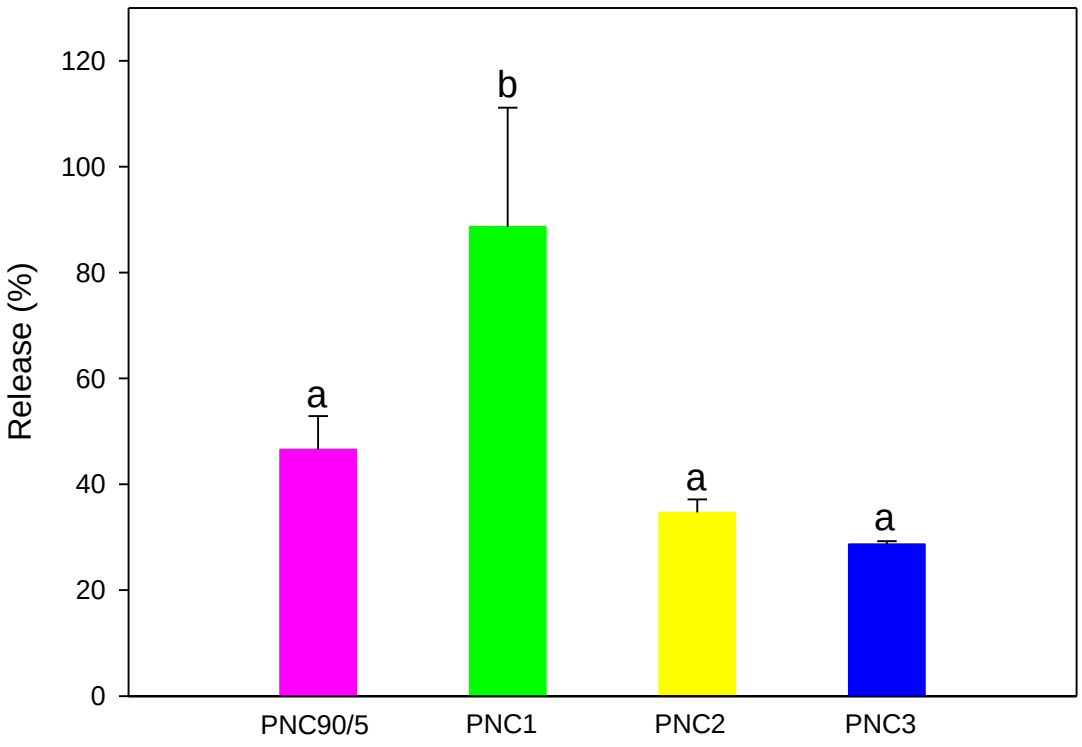

Fig. 7. *Trans*-cinnamaldehyde release at 37 ˚C for 6 h from o/w NC coated with chitosan (PNC90/5), CSder1 (PNC1), CSder2 (PNC2) and CSder3 (PNC3). Statistical differences ($p \leq 0.05$) are indicated with different numbers.

3.2.4. Stability analysis

The stability of the *t*CA-loaded o/w NC in PBS were analyzed over 24 h at 37 ºC. Thus, it could be analysed the stability of NC under more realistic physiological conditions, where media pH and ionic strength will shield electrostatic charges on the NC surfaces leading to aggregation [36,37]. According to the results, the CS-coated *t*CA-loaded o/w NC showed an increase in their size from the moment in which the NC were immersed in PBS. Two populations were recorded after 24 h. The correlation function for CS-coated *t*CA-loaded o/w NC (Fig. 8B) confirmed that there were not larger particles apart from those shown in the size plot by intensity distribution (Fig. 8A) as it was for CSder1- and CSder2-coated *t*CA-loaded o/w NC (Fig.s 8D and F, respectively). In these cases, the o/w

NC showed aggregation immediately after the immersion in PBS (Fig.s 8C and E, respectively). Besides, the intercept of the correlation function for the measurement after 24 h of incubation became greater than 1.0, revealing the presence of very large structures in the sample. Similar results have been previously reported for colloidal suspensions when exposed to neutral pH and increased ionic strength [37,38]. Surprisingly, the measurement for CSder3-coated *t*CA-loaded o/w NC showed no aggregation during the first 24 h of incubation in PBS (Fig. 8G and H). It seems that the CSder3 stabilizes the o/w NC sterically. The reasons to support this hypothesis are that the charges on the ammonium group would be screened by the ionic strength (0.01 M) and that the differences observed among different CS derivatives used stem on the length of side chain. It is plausible to hypothesize that the side chains of CSder1 and CSder2 were not long enough to prevent the aggregation process. Future studies will address the validity of this proposal in greater detail.

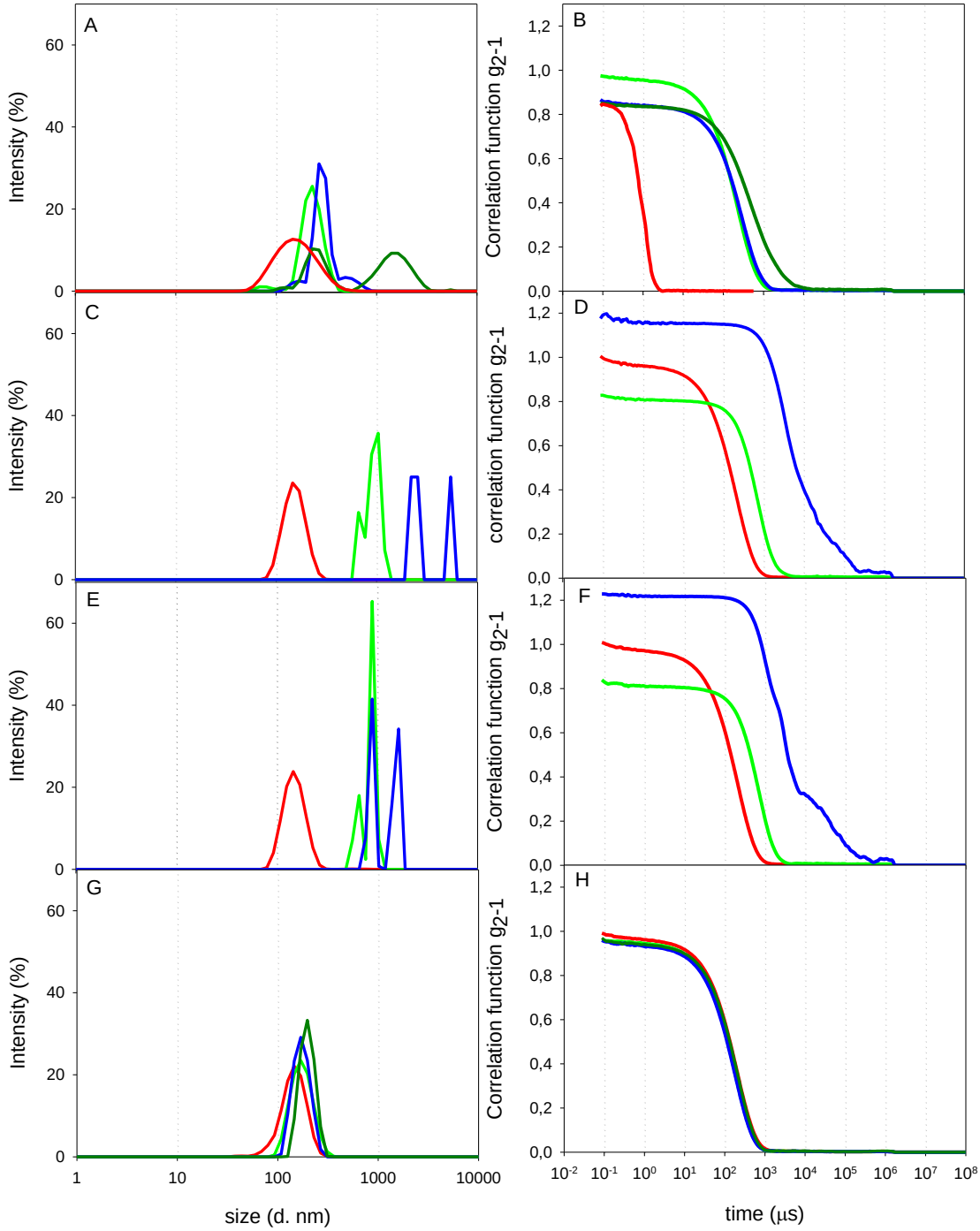

Fig. 8. Stability of o/w NC in PBS. The plots represent size by intensity distribution (A, C, E, G) and correlation functions (B, D, F, H) of o/w NC coated with chitosan (A, B), CSder1 (C, D), CSder2 (E, F) and CSder3 (G, H). The curves represent the average of the measurements carried out before adding the o/w NC into PBS (red) or immediately after adding into PBS (light green) or after 3 h (blue) or 24 h (dark green) of adding to PBS.

4. Conclusions

Trans-cinnamaldehyde, an effective anti-QS compound with potential use in the treatment against multi-resistant bacterial strains, has been successfully loaded into o/w NC coated with CS and a series of different quaternized ammonium CS-derivatives of varying side chain length. The quaternary ammonium CS-derivatives were synthesized using a novel and direct chemical approach to yield high DS in the products. The highest *t*CA loading capacity and release corresponded to CSder1-coated o/w NC. The o/w NC comprising CS, CSder1, CSder2 showed immediate aggregation upon incubation in PBS, presumably driven by the electrostatic screening of the surface charge. By contrast, the CSder3-coated *t*CA-loaded o/w NC showed stability in this medium. Future studies will address the stability and *t*CA kinetics of release from o/w NC in bacterial culture media and their AHL-regulated anti-QS activity in relevant bacterial models.

5. Author contributions

Conceptualization: FMG; PS and MCG; Funding acquisition: FMG; Investigation: MCG PS and SB; Methodology: MCG, SB, YGE and GK; Supervision: FMG; Writing original draft: MCG, SB, YGE, GK, PS and FMG. All authors have read and agreed to the published version of the manuscript.

6. Declarations of interest

None.

7. Acknowledgements

MCG acknowledges for the fellowship for postdoctoral training (20381/PD/17) funded by the Consejería de Empleo, Universidades y Empresa de la CARM, through the Fundación Séneca de la Región de Murcia and the funding received funding form the European Union's Horizon 2020 research and innovation programme under the Marie

Sklodowska-Curie (grant agreement No 101024387). GK acknowledges for the Newton International Fellowship (NIF\RI\180856) from the Academy of Medical Sciences, United Kingdom. SB was beneficiary of a bursary from the EU ERASMUS scheme.

8. Funding

This research did not receive any specific grant from funding agencies in the public, commercial, or non-for-profit sectors.

9. Reference list

[1] X. Qin, T. Kräft, F.M. Goycoolea, Chitosan encapsulation modulates the effect of trans-cinnamaldehyde on AHL-regulated quorum sensing activity, Colloids Surfaces B Biointerfaces. 169 (2018) 453–461. https://doi.org/10.1016/j.colsurfb.2018.05.054.

[2] H. Li, Q. Shen, W. Zhou, H. Mo, D. Pan, L. Hu, Nanocapsular dispersion of cinnamaldehyde for enhanced inhibitory activity against aflatoxin production by Aspergillus flavus, Molecules. 20 (2015) 6022–6032. https://doi.org/10.3390/molecules20046022.

[3] V. Tiwari, R. Roy, M. Tiwari, Antimicrobial active herbal compounds against Acinetobacter baumannii and other pathogens, Front. Microbiol. 6 (2015). https://doi.org/10.3389/fmicb.2015.00618.

[4] C. Niu, S. Afre, E.S. Gilbert, Subinhibitory concentrations of cinnamaldehyde interfere with quorum sensing, Lett. Appl. Microbiol. 43 (2006) 489–494. https://doi.org/10.1111/j.1472-765X.2006.02001.x.

[5] A.A. Doyle, J.C. Stephens, A review of cinnamaldehyde and its derivatives as antibacterial agents, Fitoterapia. 139 (2019). https://doi.org/10.1016/j.fitote.2019.104405.

[6] N.G. Vasconcelos, J.H.F. De Sá Queiroz, K.E. Da Silva, P.C. De Paula

503 Vasconcelos, J. Croda, S. Simionatto, Synergistic effects of Cinnamomum cassia
504 L. essential oil in combination with polymyxin B against carbapenemase-
505 producing Klebsiella pneumoniae and Serratia marcescens, PLoS One. 15 (2020).
506 https://doi.org/10.1371/journal.pone.0236505.
507 [7] S.H. Topa, E.A. Palombo, P. Kingshott, L.L. Blackall, Activity of cinnamaldehyde
508 on quorum sensing and biofilm susceptibility to antibiotics in Pseudomonas
509 aeruginosa, Microorganisms. 8 (2020).
510 https://doi.org/10.3390/microorganisms8030455.
511 [8] S.A.K.S. Ahmed, M. Rudden, T.J. Smyth, J.S.G. Dooley, R. Marchant, I.M. Banat,
512 Natural quorum sensing inhibitors effectively downregulate gene expression of
513 Pseudomonas aeruginosa virulence factors, Appl. Microbiol. Biotechnol. (2019).
514 https://doi.org/10.1007/s00253-019-09618-0.
515 [9] Y. Turovskiy, D. Kashtanov, B. Paskhover, M.L. Chikindas, Quorum Sensing:
516 Fact, Fiction, and Everything in Between, Adv. Appl. Microbiol. 62 (2007) 191–
517 234. https://doi.org/10.1016/S0065-2164(07)62007-3.
518 [10] B.L. Bassler, R. Losick, Bacterially Speaking, Cell. 125 (2006) 237–246.
519 https://doi.org/10.1016/j.cell.2006.04.001.
520 [11] D. Deryabin, A. Galadzhieva, D. Kosyan, G. Duskaev, Plant-derived inhibitors of
521 AHL-mediated quorum sensing in bacteria: Modes of action, Int. J. Mol. Sci. 20
522 (2019). https://doi.org/10.3390/ijms20225588.
523 [12] R. Watkins, L. Wu, C. Zhang, R.M. Davis, B. Xu, Natural product-based
524 nanomedicine: Recent advances and issues, Int. J. Nanomedicine. 10 (2015) 6055–
525 6074. https://doi.org/10.2147/IJN.S92162.
526 [13] F. Donsì, M. Annunziata, M. Vincensi, G. Ferrari, Design of nanoemulsion-based
527 delivery systems of natural antimicrobials: Effect of the emulsifier, J. Biotechnol.

159 (2012) 342–350. https://doi.org/10.1016/j.jbiotec.2011.07.001.

[14] A. Sedaghat Doost, K. Dewettinck, F. Devlieghere, P. Van der Meeren, Influence of non-ionic emulsifier type on the stability of cinnamaldehyde nanoemulsions: A comparison of polysorbate 80 and hydrophobically modified inulin, Food Chem. 258 (2018) 237–244. https://doi.org/10.1016/j.foodchem.2018.03.078.

[15] F. Froiio, L. Ginot, D. Paolino, N. Lebaz, A. Bentaher, H. Fessi, A. Elaissari, Essential oils-loaded polymer particles: Preparation, characterization and antimicrobial property, Polymers (Basel). 11 (2019). https://doi.org/10.3390/polym11061017.

[16] P.D.S. Chaves, L.A. Frank, A.G. Frank, A.R. Pohlmann, S.S. Guterres, R.C.R. Beck, Mucoadhesive Properties of Eudragit®RS100, Eudragit®S100, and Poly(ε-caprolactone) Nanocapsules: Influence of the Vehicle and the Mucosal Surface, AAPS PharmSciTech. 19 (2018) 1637–1646. https://doi.org/10.1208/s12249-018-0968-5.

[17] X. Lang, T. Wang, M. Sun, X. Chen, Y. Liu, Advances and applications of chitosan-based nanomaterials as oral delivery carriers: A review, Int. J. Biol. Macromol. 154 (2020) 433–445. https://doi.org/10.1016/j.ijbiomac.2020.03.148.

[18] R.A. Bapat, C.P. Joshi, P. Bapat, T. V. Chaubal, R. Pandurangappa, N. Jnanendrappa, B. Gorain, S. Khurana, P. Kesharwani, The use of nanoparticles as biomaterials in dentistry, Drug Discov. Today. 24 (2019) 85–98. https://doi.org/10.1016/j.drudis.2018.08.012.

[19] X. Qin, J. Emich, F.M. Goycoolea, Assessment of the quorum sensing inhibition activity of a non-toxic chitosan in an N-Acyl homoserine lactone (AHL)-based Escherichia coli biosensor, Biomolecules. 8 (2018). https://doi.org/10.3390/biom8030087.

553 [20] L. von Palubitzki, Y. Wang, S. Hoffmann, S. Vidal-y-Sy, B. Zobiak, A. V. Failla,
554 P. Schmage, A. John, A. Osorio-Madrazo, A.T. Bauer, S.W. Schneider, F.M.
555 Goycoolea, C. Gorzelanny, Differences of the tumour cell glycocalyx affect
556 binding of capsaicin-loaded chitosan nanocapsules, Sci. Rep. 10 (2020) 1–16.
557 https://doi.org/10.1038/s41598-020-79882-y.
558 [21] X. Qin, C. Engwer, S. Desai, C. Vila-Sanjurjo, F.M. Goycoolea, An investigation
559 of the interactions between an E. coli bacterial quorum sensing biosensor and
560 chitosan-based nanocapsules, Colloids Surfaces B Biointerfaces. 149 (2017) 358–
561 368. https://doi.org/10.1016/j.colsurfb.2016.10.031.
562 [22] E.O. Omwenga, A. Hensel, A. Shitandi, F.M. Goycoolea, Chitosan
563 nanoencapsulation of flavonoids enhances their quorum sensing and biofilm
564 formation inhibitory activities against an E.coli Top 10 biosensor, Colloids
565 Surfaces B Biointerfaces. 164 (2018) 125–133.
566 https://doi.org/10.1016/j.colsurfb.2018.01.019.
567 [23] H.T. Nguyen, A. Hensel, F.M. Goycoolea, Chitosan/cyclodextrin surface-adsorbed
568 naringenin-loaded nanocapsules enhance bacterial quorum quenching and anti-
569 biofilm activities, Colloids Surfaces B Biointerfaces. 211 (2022) 112281.
570 https://doi.org/10.1016/j.colsurfb.2021.112281.
571 [24] M. Rinaudo, G. Pavlov, J. Desbrières, Influence of acetic acid concentration on the
572 solubilization of chitosan, Polymer (Guildf). 40 (1999) 7029–7032.
573 https://doi.org/10.1016/S0032-3861(99)00056-7.
574 [25] P. Sahariah, M. Másson, Antimicrobial Chitosan and Chitosan Derivatives: A
575 Review of the Structure-Activity Relationship, Biomacromolecules. 18 (2017)
576 3846–3868. https://doi.org/10.1021/acs.biomac.7b01058.
577 [26] P. Calvo, C. Remuñán-López, J.L. Vila-Jato, M.J. Alonso, Development of

positively charged colloidal drug carriers: Chitosan-coated polyester nanocapsules and submicron-emulsions, Colloid Polym. Sci. 275 (1997) 46–53. https://doi.org/10.1007/s003960050050.

[27] B. Duncan, X. Li, R.F. Landis, S.T. Kim, A. Gupta, L.S. Wang, R. Ramanathan, R. Tang, J.A. Boerth, V.M. Rotello, Nanoparticle-Stabilized Capsules for the Treatment of Bacterial Biofilms, ACS Nano. 9 (2015) 7775–7782. https://doi.org/10.1021/acsnano.5b01696.

[28] R.R. Gadkari, S. Suwalka, M.R. Yogi, W. Ali, A. Das, R. Alagirusamy, Green synthesis of chitosan-cinnamaldehyde cross-linked nanoparticles: Characterization and antibacterial activity, Carbohydr. Polym. 226 (2019). https://doi.org/10.1016/j.carbpol.2019.115298.

[29] B.I. Andreica, X. Cheng, L. Marin, Quaternary ammonium salts of chitosan. A critical overview on the synthesis and properties generated by quaternization, Eur. Polym. J. 139 (2020) 110016. https://doi.org/10.1016/j.eurpolymj.2020.110016.

[30] B.E. Benediktsdóttir, V.S. Gaware, Ö. V. Rúnarsson, S. Jónsdóttir, K.J. Jensen, M. Másson, Synthesis of N,N,N-trimethyl chitosan homopolymer and highly substituted N-alkyl-N,N-dimethyl chitosan derivatives with the aid of di-tert-butyldimethylsilyl chitosan, Carbohydr. Polym. 86 (2011) 1451–1460. https://doi.org/10.1016/j.carbpol.2011.06.007.

[31] P. Sahariah, V.S. Gaware, R. Lieder, S. Jónsdóttir, M. Hjálmarsdóttir, O.E. Sigurjonsson, M. Másson, The effect of substituent, degree of acetylation and positioning of the cationic charge on the antibacterial activity of quaternary chitosan derivatives, Mar. Drugs. 12 (2014) 4635–4658. https://doi.org/10.3390/md12084635.

[32] Ö.V. Rúnarsson, J. Holappa, T. Nevalainen, M. Hjálmarsdóttir, T. Järvinen, T.

603 Loftsson, J.M. Einarsson, S. Jónsdóttir, M. Valdimarsdóttir, M. Másson,
604 Antibacterial activity of methylated chitosan and chitooligomer derivatives:
605 Synthesis and structure activity relationships, Eur. Polym. J. 43 (2007) 2660–2671.
606 https://doi.org/10.1016/j.eurpolymj.2007.03.046.
607 [33] Y. González-Espinosa, B. Sabagh, E. Moldenhauer, P. Clarke, F.M. Goycoolea,
608 Characterisation of chitosan molecular weight distribution by multi-detection
609 asymmetric flow-field flow fractionation (AF4) and SEC, Int. J. Biol. Macromol.
610 136 (2019) 911–919. https://doi.org/10.1016/j.ijbiomac.2019.06.122.
611 [34] F.M. Goycoolea, V. Milkova, Electrokinetic behavoir of chitosan adsorbed on o/w
612 nanoemulsion droplets, Colloids Surfaces A Physicochem. Eng. Asp. 519 (2017)
613 205–211. https://doi.org/10.1016/j.colsurfa.2016.05.093.
614 [35] P. Calvo, J.L. Vila-Jato, M.J. Alonso, Evaluation of cationic polymer-coated
615 nanocapsules as ocular drug carriers, Int. J. Pharm. 153 (1997) 41–50.
616 https://doi.org/10.1016/S0378-5173(97)00083-5.
617 [36] G. Trefalt, F.J.M. Ruiz-Cabello, M. Borkovec, Interaction forces,
618 heteroaggregation, and deposition involving charged colloidal particles, J. Phys.
619 Chem. B. 118 (2014) 6346–6355. https://doi.org/10.1021/jp503564p.
620 [37] M.J. Santander-Ortega, J.M. Peula-García, F.M. Goycoolea, J.L. Ortega-Vinuesa,
621 Chitosan nanocapsules: Effect of chitosan molecular weight and acetylation degree
622 on electrokinetic behaviour and colloidal stability, Colloids Surfaces B
623 Biointerfaces. 82 (2011) 571–580. https://doi.org/10.1016/j.colsurfb.2010.10.019.
624 [38] M. Collado-González, M. Cristina Ferreri, A.R. Freitas, A.C. Santos, N.R.
625 Ferreira, G. Carissimi, J.A.D. Sequeira, F. Guillermo Díaz Baños, G. Villora, F.
626 Veiga, A. Ribeiro, Complex polysaccharide-based nanocomposites for oral insulin
627 delivery, Mar. Drugs. 18 (2020) 1–18. https://doi.org/10.3390/md18010055.